2

Medial Axis

2.1 Introduction

The medial axis [24] transform associates a skeleton-like structure to a shape, which encodes its geometry. The medial axis itself (or skeleton) is the center of discs of maximal radii inscribed in the shape. The medial axis transform stores in addition the maximal radii.

More precisely, represent a shape by an open connected bounded set in the plane, denoted Ω. Let $B(p,r)$ denote the open disc of center $p \in \mathbb{R}^2$ and radius $r > 0$. One says that such a disc is maximal in Ω if and only if it is included in Ω, and no disc in which it is (strictly) contained is included in Ω. The skeleton of Ω, denoted $\Sigma(\Omega)$, is the set of all p such that $B(p,r)$ is maximal in Ω for some $r > 0$, i.e., $\Sigma(\Omega)$ is the set of loci of the centers of maximal discs. We shall also denote $\Sigma^*(\Omega)$ as the set of pairs (p,r) such that $B(p,r)$ is maximal. This is the medial axis transform (MAT). We have the following proposition.

Proposition 2.1. *The medial axis transform, $\Sigma^*(\Omega)$, uniquely characterizes Ω.*

Proof. Let

$$\tilde{\Omega} = \bigcup_{(p,r)\in\Sigma^*(\Omega)} B(p,r).$$

By definition of Σ^*, we have $\tilde{\Omega} \subset \Omega$ and we want to prove the reverse inclusion.

For $x \in \Omega$, let $r_x = \operatorname{dist}(x, \Omega^c)$ so that $b(x, r_x) \subset \Omega$ and define

$$G_x = \{y \in \Omega : B(y, r_y) \supset B(x, r_x)\}$$

and $r_x^* = \sup r_y, y \in G_x$. By definition, there exists a sequence (y_n) such that $r_{y_n} \to r_x^*$, and, since Ω is bounded, we can assume (replacing y_n by a subsequence is needed) that $y_n \to y^* \in \overline{\Omega}$. Obviously, y^* cannot belong to $\partial\Omega$ since this would imply $r_{y_n} \to 0$ and $r_x^* \geq r_x > 0$ (since $x \in G_x$). Also, since

$B(y_n, r_{y_n}) \subset \Omega$, we have at the limit $B(y^*, r_x^*) \subset \overline{\Omega}$ which implies $B(y^*, r_x^*) \subset \Omega$ because Ω is open. Similarly, passing to the limit in the inclusion $B(x, r_x) \subset B(y_n, r_{y_n})$ implies $x \in B(y^*, r_x^*)$.

We now show that $B(y^*, r_x^*)$ is maximal, which will prove that $\Omega \subset \tilde{\Omega}$, since we started with an arbitrary $x \in \Omega$. But if $B(y^*, r_x^*)$ is included in some ball $B(y, r) \in \Omega$, it will be a fortiori included in $B(y, r_y)$ and since $x \in B(y^*, r_x^*)$, we see that y must be in G_x with $r_y > r_x^*$, which is a contradiction.

2.2 Structure of the Medial Axis

We assume that Ω is the interior of a piecewise smooth Jordan curve. Some structural properties of the skeleton can be obtained under some assumptions on the regularity of the curve [46]. The assumption is that the smooth arcs are analytic, which means infinitely differentiable, and such for each t, $m(t)$ is the limit of its Taylor series, except at a finite number of points; for these exceptional points, it is required that m has both left and right tangents. The simplest example of a curve satisfying this assumption is a polygon.

For such a curve, it can be shown that all but a finite number of points in the skeleton are such that the maximal disc $B(p, r)$ meets the curve m at exactly two points. Such points on the skeleton are called regular. Non-regular points separate into three categories.

The first type is when the maximal disc, $B(m, r)$, meets the curve in more than two connected regions. Such points are *bifurcation points* of the skeleton. The second possibility is when there is only one connected component; then, there are two possibilities: either m is the center of an osculating circle to the curve, or there exists a concave angle at the intersection of the curve and the maximal disc. The third possibility is when there are two connected components, but one of them is a sub-arc of the curve. This happens only when the curve has circular arcs.

The skeleton itself is connected, and it is composed of a finite number of smooth curves.

2.3 The Skeleton of a Polygon

There are at least two reasons for which the skeletons of polygons have practical interest. The first one is that digital shapes can always be considered as polygons (because they are described by a finite number of points), and numerical algorithms for skeleton computation rely on the description of the skeletons of polygons. The second one is that truly polygonal shapes (not only at the discretization level) are very common, because man-made objects often are polyhedrons.

Consider a closed polygon, without self-intersections. Denote its vertices $m_1, \ldots, m_N, m_{N+1} = m_1$. Let s_i denote the ith edge, represented by open line

segments (m_i, m_{i+1}), for $i = 1, \ldots, N$. A maximal disc within the polygon has to meet the boundary at two points. We separate the cases depending on whether these points are on edges or vertices.

Let $B(m, r)$ be a maximal disc. Assume first that it is tangent to s_i at some point $p \in s_i$. Denote $T_i = (m_{i+1} - m_i)/|m_{i+1} - m_i|$ the unit tangent to s_i and N_i the unit normal. We assume that the orientation is such that N_i points inward. We must have

$$p = m - rN_i \text{ and } p = m_i + tT_i$$

for some $t \in (0, |m_{i+1} - m_i|)$. Taking the dot product of both equations with T_i and computing the difference yields

$$t = (m - m_i)^T T_i.$$

We therefore obtain the fact that $B(m, r)$ is tangent to s_i if and only if

$$m - rN_i = m_i + ((m - m_i)^T T_i)T_i \quad \text{with } 0 \leq (m - m_i)^T T_i \leq |m_{i+1} - m_i|.$$

We can distinguish three types of maximal discs: $B(m, r)$.

1. Bitangents: there exists $i \neq j$ with

$$m = m_i + ((m - m_i)^T T_i)T_i + rN_i = m_j + ((m - m_j)^T T_j)T_j + rN_j \text{ and}$$
$$0 \leq (m - m_i)^T T_i \leq |m_{i+1} - m_i|, 0 \leq (m - m_j)^T T_j \leq |m_{j+1} - m_j|.$$

2. Discs that meet the boundary at exactly one edge and one vertex: there exists $i \neq j$ such that

$$\begin{aligned} m &= m_i + ((m - m_i)^T T_i)T_i + rN_i, \\ &\quad 0 \leq ((m - m_i)^T)T_i \leq |m_{i+1} - m_i| \\ &\text{and } |m - m_j| = r. \end{aligned}$$

3. Discs that meet the boundary at two vertices: there exists $i \neq j$ such that $|m - m_i| = |m - m_j| = r$.

Note that a maximal ball can meet a vertex only if this vertex points inward (concave vertex). In particular, with convex polygons, only the first case can happen.

The interesting consequence of this result is that the skeleton of a polygon is the union of line segments and arcs of parabola. To see this, consider the equations for the three previous cases. For bitangents, we have

$$r = (m - m_i)^T N_i = (m - m_j)^T N_j$$

which implies

$$(m - m_i)^T (N_j - N_i) = (m_j - m_i)^T N_j.$$

If $N_i \neq N_j$, this is the equation of a line orthogonal to $N_i - N_j$. The case $N_i = N_j$ can never occur because the normals have to point to the interior of maximal balls and therefore coincide only if $s_i = s_j$.

For the second case, we have

$$m - m_i = ((m - m_i)^T) T_i T_i + |m - m_j| N_i$$

which yields

$$(m - m_i)^T N_i = |m - m_j|.$$

This is the equation of a parabola. To see why, express m as $m = m_i + \alpha T_i + \beta N_i$. The previous equations yield $\beta \geq 0$ and

$$\beta^2 = (\alpha - (m_j - m_i)^T T_i)^2 + (\beta - (m_j - m_i)^T N_i)^2$$

or

$$2(m_j - m_i)^T N_i \beta = (\alpha - (m_j - m_i)^T T_i)^2 + ((m_j - m_i)^T N_i)^2.$$

Finally, in the last case, the skeleton coincides with the line of points which are equidistant from the two vertices. We have therefore proved the following fact (which comes in addition to the properties discussed in Section 2.2).

Proposition 2.2. *The skeleton of a polygonal curve is a union of line segments and parabolas. For a convex polygon, the skeleton only contains line segments.*

2.4 Voronoï Diagrams

2.4.1 Voronoï Diagrams of Line Segments

The previous computation and the most efficient algorithms to compute skeletons are related by the theory of Voronoï diagrams. We start with their definition:

Definition 2.3. *Let $F_1, \ldots F_N$ be closed subsets of $\mathbb{R}^2$. The associated Voronoï cells are the sets $\Omega_1, \ldots, \Omega_N$ defined by*

$$x \in \Omega_i \Leftrightarrow d(x, F_i) < \min_{j \neq i} d(x, F_j).$$

The union of the boundaries, $\bigcup_{i=1}^N \partial\Omega_i$, forms the Voronoï diagram associated to $F_1, \ldots, F_N$.

In the case of a polygonal curve, the skeleton is included in the Voronoï diagram of the closed line segments that form the curve. A point of the skeleton has indeed to meet at least two segments (sometimes at their common vertices), and is at a strictly larger distance from the ones it does not intersect. It therefore belongs to the boundary of the cells. The converse is false: a point from the diagram is not necessarily in the skeleton (some points may correspond to external balls).

There exist very efficient algorithms to compute these diagrams. We shall not detail them here, but references can be found in [166, 159].

The notion of Voronoï diagrams for a polygon can be extended to a general curve. The question is to find sub-arcs $F_1, \ldots, F_N$ of the curve with the property that their diagram contains the curve's skeleton. What we have said concerning polygons applies, except in one case: when a maximal disc meets an arc at two distinct points. This could not happen with straight lines, and a condition ensuring that this does not happen for a given arc is as follows [126]. Recall that a vertex of a smooth curve m is a local extremum of the curvature.

Theorem 2.4. *A sub-arc of a C^2 closed curve which has two points belonging to a maximal disc necessarily contains a vertex.*

Therefore, it suffices to cut the curve at vertices to be sure that the obtained arcs cannot hold two contacts with maximal discs.

2.4.2 Voronoï Diagrams of the Vertices of Polygonal Curves

The medial axis can, in some sense, also be interpreted as the skeleton of the infinite family of points in the curve. This leads to the question of whether the Voronoï diagram of the sequence of points in a discrete curve is a good approximation of the skeleton when the discretization step goes to 0. The answer is: not at all, and almost yes.

The cells of the Voronoï diagram of a finite family of points are polygons, which makes them even simpler than the diagram of line segments. Moreover, there is an extensive literature on their computation, which is one of the basic algorithms in discrete and computational geometry [166, 162].

In the diagram of a polygonal curve, there are essentially two types of segments: those containing points which are equidistant to two consecutive vertices, and the rest. When the discretization is fine enough, the first type of segments cannot belong to the skeleton, and have to be pruned out of the Voronoï diagram. They are easily detectable, since they contain the midpoint of the two consecutive vertices, and therefore cross the curve. The computation of the skeleton of a discrete curve can therefore be done as follows: first compute the Voronoï diagram of the vertices. Then remove the segments that are not entirely in the interior of the curve. Figure 2.1 illustrates how discretization affects the skeleton in a simple example.

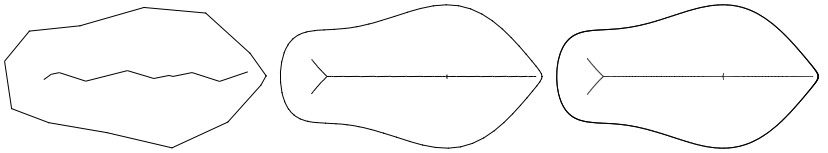

Fig. 2.1. Comparison of medial axes computed using Voronoï diagrams with different degrees of discretization.

2.5 Thinning

Thinning algorithms create their own kind of skeleton which does not necessarily correspond to the centers of maximal discs. They are, however, quite efficient and generally easy to implement. The principle is to progressively "peel" the boundary of the region until only a skeletal structure remains. One of the first methods is the Hilditch algorithm [111], in which a sequence of simple tests are performed to decide whether a pixel must be removed or not from the region. Another similar point of view uses the erosion operation in mathematical morphology [182]. We briefly describe the latter.

Define a structuring element B to be a symmetric subset of $\mathbb{R}^2$ (for example a small disc centered at 0). Using B, we define a sequence of operators that apply to a set X and creates a new set:

$$\begin{aligned} E_B(X) &= \{x : x + B \subset X\} \text{ (erosion)}, \\ D_B(X) &= \{x : x + B \cap X \neq \emptyset\} \text{ (dilation)}, \\ O_B(X) &= D_B \circ E_B(X) \text{ (opening)}, \\ L_B(X) &= X \setminus O_B(X). \end{aligned}$$

Erosion is like peeling X with a knife shaped like B. Dilation spreads matter around X, with a thickness once again provided by B. Opening is an erosion followed by a dilation, which essentially puts back what the erosion has removed, except the small structures which have completely been removed and cannot be recovered (since there is nothing left to spread on). The last operation, L_B, precisely collects these lost structures (called linear parts), and is the basic operator for the morphological skeleton which is defined by

$$S(X) = \cup_{n=1}^{N} L_B(E_{nB}(X)).$$

This is the union of the linear parts of X after successive erosions.

2.6 Sensitivity to Noise

One of the main issues with the medial axis transform is its lack of robustness to noise. Figure 2.2 provides an example of how small variations at the

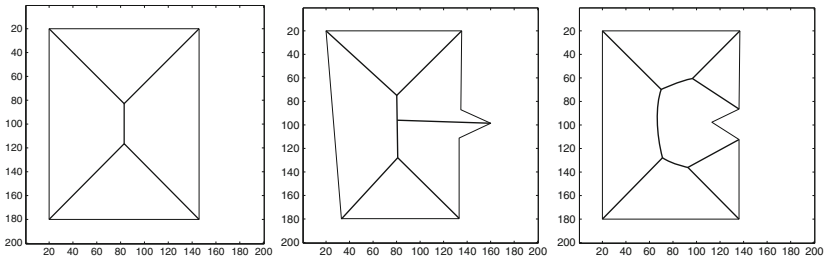

Fig. 2.2. Effect of a small shape change in the boundary on the skeleton of a rectangular shape.

boundary of a shape can result in dramatic changes in the skeleton. In fact, we have seen in our discussion of polygons that the addition of a convex vertex automatically results in a branch in the skeleton reaching to it.

Because of this, many skeletonization algorithms come with a way to prune the skeleton of spurious branches. There are two ways to do this.

- *Prior smoothing of the curve.* Curve smoothing algorithms have been described in Section 6. For polygons, smoothing can be done by removing small structures of flattening vague angle. It is interesting to note that smoothing curves does not always result in simplifying the skeleton (see [16] for a discussion).
- *Pruning.* Branches can be removed after the computation of the skeleton. This can be based on several principles, since branches resulting from small incidents at the boundary can be detected on the skeleton [93].

2.7 Recovering the Initial Curve

Given a parametrized sub-arc of the medial axis transform, one can explicitly reconstruct the part of the boundary $\partial\Omega$ which is associated to it (the contact points of the maximal balls with $\partial\Omega$). Assume that a C^1 function γ, from (a, b) to $\Sigma^*(\Omega)$ is given. Denote $\gamma(u) = (m(u), r(u))$.

Without loss of generality, assume that $u \mapsto m(u)$ is arc length ($|\dot{m}_u| = 1$). Assume also that $B(m(u), r(u))$ has exactly two contacts with $\partial\Omega$ (this is typically true on $\Sigma^*(\Omega)$ except at a finite number of points).

If $x \in \partial\Omega \cap B(m(u), r(u))$, then $|x - m(u)| = r(u)$ and, for all $\varepsilon \neq 0$, $|x - m(u + \varepsilon)| \geq r(u + \varepsilon)$ (because $B(m(u + \varepsilon), r(u + \varepsilon)) \subset \Omega$). Thus, letting $f(\varepsilon) = |x - m(u + \varepsilon)|^2 - r(u + \varepsilon)^2$, we have $f(0) = \partial_\varepsilon f(0) = 0$, with

$$\partial_\varepsilon f(0) = -2\big\langle x - m(u)\,,\, \dot{m}_u(u)\big\rangle + 2r(u)\dot{r}_u(u).$$

Solving this equation, we obtain two solutions for x, given by

$$x_+(u) = m(u) + r(u)\left[-\dot{r}_u(u)\dot{m}_u(u) + \sqrt{1-\dot{r}_u(u)^2}q(u)\right],$$
$$x_-(u) = m(u) + r(u)\left[-\dot{r}_u(u)\dot{m}_u(u) - \sqrt{1-\dot{r}_u(u)^2}q(u)\right],$$

with $q(u) \perp \dot{m}_u(u)$, $|q(u)| = 1$. Note that this computation shows that $|\dot{r}_u| < 1$ is a necessary condition for the existence of two distinct solutions.

The curvature of the boundary can also be related to the medial axis via an explicit formula. Let ρ_+ (resp. ρ_-) be the vector $-\dot{r}_u\dot{m}_u + \sqrt{1-\dot{r}_u^2}q$ (resp. $-\dot{r}_u\dot{m}_u - \sqrt{1-\dot{r}_u^2}q$) so that $x_+ = m + r\rho_+$ and $x_- = m + r\rho_-$. The following discussion holds for both arcs and we temporarily drop the $+$ and $-$ indices in the notation.

We have $x = m + r\rho$; ρ is a unit vector, and since the maximum disc is tangent to the curve at x, ρ is normal to the curve. Since r is positive and ρ is a radial vector for a maximal disc, ρ points outward from the curve at point x and therefore is oriented in the opposite direction to the normal (assuming that the curve is positively oriented). Introduce the vector $h = \dot{m}_u + \dot{r}_u\rho$. We have $h^T\rho = -\dot{r}_u + \dot{r}_u = 0$ so that h is orthogonal to ρ. Since $|\rho| = 1$, $\dot{\rho}_u$ is also orthogonal to ρ and there exists a number c such that $\dot{\rho}_u = -ch$ (we have $|h|^2 = 1 - \dot{r}_u^2 > 0$ so that $h \neq 0$). Since $\rho = -N$, we also have

$$\dot{\rho}_u = \dot{\rho}_s\frac{ds}{du} = \kappa\frac{ds}{du}T$$

where κ is the curvature of the considered arc of curve. Likewise, $\dot{x}_u = (ds/du)T$ so that $\dot{\rho}_u = \kappa\dot{x}_u$. We now use this relation to compute κ: we have $\dot{x}_u = \dot{m}_u + \dot{r}_u\rho + r\dot{\rho}_u = (1 - cr)h$. This implies

$$\kappa = -c/(1 - cr)$$

which provides a very simple relation between c and the curvature.

To be complete, it remains to compute c. From $\dot{\rho}_u = -c(\dot{m}_u + \dot{r}_u\rho)$, we get

$$\dot{\rho}_u^T\dot{m}_u = -c(1 + \dot{r}_u\rho^T\dot{m}_u) = -c(1 - \dot{r}_u^2).$$

We also have

$$-\ddot{r}_{uu} = \partial_u(\rho^T\dot{m}_u) = \dot{\rho}_u^T\dot{m}_u + \rho^T\ddot{m}_{uu} = \dot{\rho}_u^T\dot{m}_u + K\rho^Tq$$

where K is the curvature of the skeleton. Writing $\rho^Tq = \varepsilon\sqrt{1-\dot{r}_u^2}$ with $\varepsilon = \pm 1$, we get the equation:

$$\dot{\rho}_u^T\dot{m}_u = -\ddot{r}_{uu} - \varepsilon K\sqrt{1-\dot{r}_u^2}$$

which yields (reintroducing the $+$ and $-$ subscripts for each contact) $c_+ = \ddot{r}_{uu}/(1-\dot{r}_u^2) + K/\sqrt{1-\dot{r}_u^2}$ and $c_- = \ddot{r}_{uu}/(1-\dot{r}_u^2) - K/\sqrt{1-\dot{r}_u^2}$.

2.8 Generating Curves from Medial and Skeletal Structures

The previous section described how to retrieve a curve once its medial axis transform has been computed. We want here to discuss the issue of specifying a curve by providing the medial axis transform.

This is a more difficult problem, because not any combination of curves and radii is a valid medial axis. Even when the skeleton consists of only one curve, we have already seen conditions in the above section, like $|\dot{r}_u| < 1$ at all points in the interior of the medial curve, that are required in the skeletal representation. We must also ensure that the specified curve is regular on both sides of the axis, which, since $\dot{x}_u = (1 - cr)h$, must ensure that $1 - cr$ does not vanish along the curve. In fact, $1 - cr$ must be positive. To see this, note that we have proved that $1 - cr = (1 - r\kappa)^{-1}$. At a convex point ($\kappa > 0$), r must be smaller than the radius of curvature $1/\kappa$ so that $1 - r\kappa > 0$. Since points of positive curvature always exist, we see that $1 - cr$ must remain positive along the curve in order to never be zero. Using the expression for c found in the previous section, this provides a rather complex condition:

$$1 - \frac{r\ddot{r}_{uu}}{1 - \dot{r}_u^2} > \frac{|K|r}{\sqrt{1 - \dot{r}_u^2}}. \tag{2.1}$$

To ensure continuity of the reconstructed curve when branches meet at the extremities of the axis, we need $|\dot{r}_u| = 1$ there. Also, if the medial axis has multiple branches, the corresponding parts of the curve must have the same limits on both sides. More conditions are needed to ensure that the contacts at these points are smooth. This provides a rather complicated set of constraints that must be satisfied by a generative medial axis model. This can be made feasible, however, in some simple cases, as shown in the following examples.

2.8.1 Skeleton with Linear Branches

Let's consider the situation in which each branch of the medial axis is a line segment, i.e., $K = 0$. The constraints on r are then $r > 0$, $\dot{r}_u^2 < 1$ and $r\ddot{r}_{uu} + \dot{r}_u^2 < 1$. The last inequality comes from the fact that $cr < 1 \Leftrightarrow r\ddot{r}_{uu} < 1 - \dot{r}_u^2$. Introducing $z = r^2/2$, this can also be written $\ddot{z}_{uu} < 1$.

Let's assume that $\ddot{z}_{uu} = -f$ with $f > -1$ and see what happens with the other conditions in some special cases.

Integrating twice, we find

$$\begin{aligned} \dot{z}_u(u) &= \dot{z}_u(0) - \int_0^u f(t)dt \\ z(u) &= z(0) + u\dot{z}_u(0) - \int_0^u (u - t)f(t)dt. \end{aligned} \tag{2.2}$$

Shapes with a Single Linear Branch

Start with the simplest situation in which the medial axis is composed of a single segment, say $m(u) = (u, 0)$, $u \in [0, 1]$. Since $|\dot{r}_u| = 1$ at the extremities and the medial axis cannot cross the curve, we need $r_u(0) = 1$ and $\dot{r}_u(1) = -1$. Denote

$$M_0(u) = \int_0^u f(t)dt$$
$$M_1(u) = \int_0^u tf(t)dt.$$

Using the identities $\dot{z}_u(0) = r(0)$, $\dot{z}_u(1) = -r(1)$, $z(0) = r(0)^2/2$ and $z(1) = r(1)^2/2$, we can solve (2.2) with respect to $r(0)$ and $r(1)$ to obtain:

$$r(0) = \frac{M_0(1) + M_0(1)^2/2 - M_1(1)}{1 + M_0(1)}$$
$$r(1) = M_0(1) - r(0) = \frac{M_0(1)^2/2 + M_1(1)}{1 + M_0(1)}.$$

These quantities must be positive, and we will assume that f is chosen with this property (note that the denominator is always positive since $f > -1$). These equations imply that z, and therefore m, are uniquely determined by f. Of course, this does not imply that the remaining constraints, which are (in terms of z) $z > 0$ and $\dot{z}_u^2 < 2z$ are satisfied on $(0, 1)$. Since the latter implies the former, we can concentrate on it, and introduce the function $h(u) = 2z(u) - \dot{z}_u(u)^2$. We have $h(0) = r(0)^2$ and $h(1) = r(1)^2$. Moreover,

$$\dot{h}_u = 2\dot{z}_u(1 - \ddot{z}_{uu}) = 2\dot{z}_u(1 + f).$$

Since $1 + f > 0$, $\dot{h}_u$ vanishes for $z_u = 0$, or $M_0(u) = r(0)$. Note that $\dot{h}_u(0) = 2r(0)(1 + f) > 0$ and $\dot{h}_u(1) = -2r(1)(1 + f) < 0$ so $\dot{h}_u$ changes signs over $(0, 1)$.

Also, since the extrema of h only occur when $\dot{z}_u > 0$ (and $h = 2z$ at these points), h will be positive under any condition that ensures that $z > 0$ when $\dot{z}_u = 0$, which reduces to $r(0)^2/2 + M_1(u) > 0$ whenever $M_0(u) = r(0)$.

There is an easy case: if $f > 0$, then $M_1(u) > 0$ and the condition is satisfied. Moreover, if $f > 0$, then $M_1(1) \leq M_0(1)$ also so that $r(0)$ and $r(1)$ are positive. However, as Figure 2.3 shows, interesting shapes are obtained when $f < 0$ is allowed.

Shapes with Three Intersecting Linear Branches

Let's now consider a slightly more complex example with one multiple point and three linear branches. So we have three lines, ℓ_1, ℓ_2, ℓ_3, starting from a single point p_0. Let $\ell_i = \{p_0 + uw_i, u \in [0, s_i]\}$ where w_1, w_2, w_3 are unit vectors.

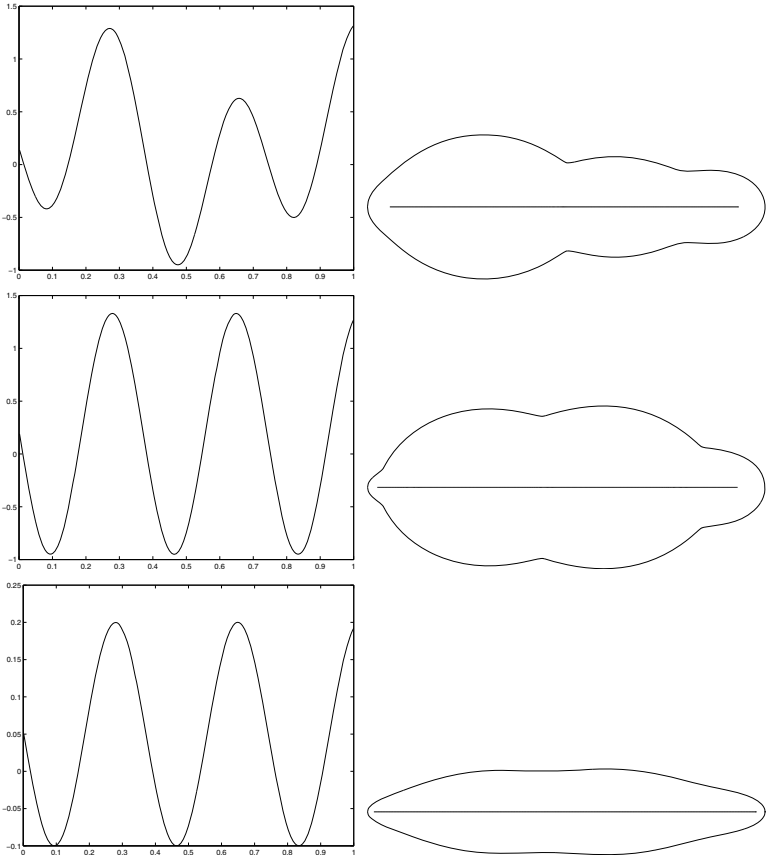

Fig. 2.3. Shapes with horizontal medial axes. The shapes are obtained with $\partial^2_{uu}(r^2) = -2f$; f is in the left column and the curves are in the right one.

Let q_i be a unit vector completing w_i in a positively oriented orthonormal frame. Finally, let $r^{(1)}, r^{(2)}$ and $r^{(3)}$ be the radii along each of these lines and $z^{(i)} = (r^{(i)})^2/2$. Assume that $\ddot{z}^{(i)}_{uu} = -f_i(u/s_i)$ for $u \in (0, s_i)$, where $f_i > -1$ as before, and is defined over $[0, 1]$.

We need to work out the compatibility conditions for the $r^{(i)}$ at the intersection point, $u = 0$. Assume that the branches are ordered so that $(w_1, w_2), (w_2, w_3)$ and (w_3, w_1) are positively oriented. The compatibility conditions are

$$x^{(1)}_+(0) = x^{(2)}_-(0),\ x^{(2)}_+(0) = x^{(3)}_-(0),\ x^{(3)}_+(0) = x^{(1)}_-(0).$$

Identifying the norms, we see that the radii must coincide: $r^{(1)}(0) = r^{(2)}(0) = r^{(3)}(0) := r_0$. So, defining h_1, h_2, h_3 by

$$h_1 = \rho_+^{(1)}(0) = \rho_-^{(2)}(0), h_3 = \rho_+^{(2)}(0) = \rho_-^{(3)}(0), h_2 = \rho_+^{(3)}(0) = \rho_-^{(1)}(0),$$

we see that the triangle $(p_0 + h_1, p_0 + h_2, p_0 + h_3)$ has p_0 as circumcenter, and the lines defining the axis are the perpendicular bisectors of its edges.

Given these remarks, it is easier to organize the construction by first specifying p_0 and the three directions h_1, h_2, h_3. This specifies the vectors w_1, w_2, w_3: given $i \in \{1, 2, 3\}$, denote the other two indices by j and j' . Then

$$w_i = (h_j + h_{j'})/|h_j + h_{j'}|$$

and, from the expression of ρ, we see that this also specifies $\dot{r}_u^{(i)}(0)$, with

$$\dot{r}_u^{(i)}(0) = -z_i^T h_j = -\frac{1}{\sqrt{2}}\sqrt{1 + h_j^T h_{j'}} = -\cos(\theta_i/2)$$

where θ_i is the angle between h_j and h'_j.

This gives, for $u \in [0, s_i]$

$$\dot{z}_u^{(i)}(u) = \dot{z}_u^{(i)}(0) - \int_0^u f^{(i)}(t/s_i)dt = -r_0 \cos\frac{\theta_i}{2} - s_i M_0^{(i)}(u/s_i)$$

and

$$z^{(i)}(u) = \frac{r_0^2}{2} - r_0 u \cos\frac{\theta_i}{2} - s_i u M_0^{(i)}(u/s_i) + s_i^2 M_1^{(i)}(u/s_i).$$

Since we need $\dot{r}_u^{(i)}(s_i) = -1$, we have $z^{(i)}(s_i) = r^{(i)}(1)^2/2$ and $\dot{z}_u^{(i)}(s_i) = -r^{(i)}(1)$. Identifying $r^{(i)}(1)^2$ in the two equations above yields

$$r_0^2 \cos^2\frac{\theta_i}{2} + 2r_0 s_i \cos\frac{\theta_i}{2} M_0^{(i)}(1) + s_i^2 M_0^{(i)}(1)^2 = r_0^2 - 2r_0 s_i \cos\frac{\theta_i}{2} - s_i^2 M_0^{(i)}(1) + s_i^2 M_1^{(i)}(1)$$

or

$$\Big(M_0^{(i)}(1)^2 + 2M_0^{(i)}(1) - 2M_1^{(i)}(1)\Big)\frac{s_i^2}{r_0^2} + 2\cos\frac{\theta_i}{2}\big(1 + M_0^{(i)}(1)\big)\frac{s_i}{r_0} - (1 - \cos^2\frac{\theta_i}{2}) = 0. \quad (2.3)$$

Assuming that $f^{(i)}$ satisfies

$$M_0^{(i)}(1)^2/2 + M_0^{(i)}(1) - M_1^{(i)}(1) > 0,$$

which a condition already encountered in the previous case, this equation has a unique solution, specifying s_i. The curve is then uniquely defined by $p_0, h_1, h_2, h_3, f^{(1)}, f^{(2)}, f^{(3)}$, with constraints on the $f^{(i)}$'s similar to those obtained in the one-branch case. Examples are provided in Figure 2.4.

Note that this construction does not really specify the medial axis, but only the orientation of its branches (since the s_i's are constrained by the rest of the parameters). One possibility to deal with this is to relax the specification of the $f_i's$ by adding a factor α_i, using

$$\ddot{z}_{uu}^{(i)} = -\alpha_i f^{(i)}.$$

This implies that $M_0^{(i)}$ and $M_1^{(i)}$ must be replaced by $\alpha_i M_0^{(i)}$ and $\alpha_i M_1^{(i)}$ in the computation above, and equation (2.3), with fixed s_i, becomes a second-degree equation in α_i. The consistency conditions (existence of a solution to this equation, requirement that $\alpha_i f^{(i)} > -1$, etc.) are, however, harder to work out in this case.

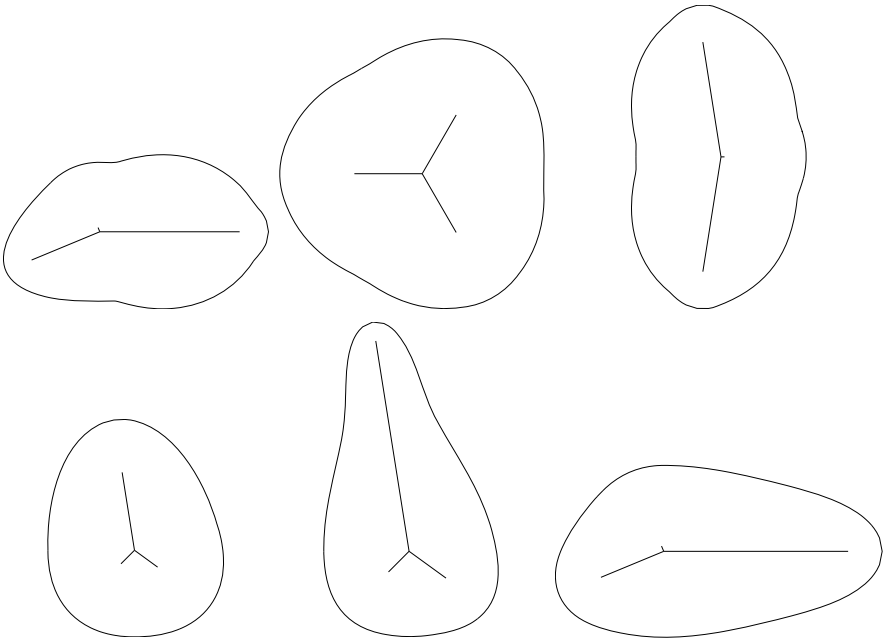

Fig. 2.4. Shapes generated from a medial axis with three linear branches.

Shapes with Generic Linear Branches

Conceptually, the above construction can be generalized to any skeleton with a ternary tree structure and linear branches. Indeed, the derivative $\dot{r}_u$ is uniquely specified at the extremities of any branch: it is -1 if the branch ends and $-\cos\theta/2$ at an intersection, where θ is specified by the branch geometry as above. Also, the radii at all branching points are uniquely specified

as soon as one of them is (the constraint propagates along the tree). Of course, as before, the fact that the solution is uniquely defined does not guarantee consistency, which become harder to specify when the structure gets more complex. Finally, it is important to note that, for all the previous methods, even if the consistency conditions are satisfied, there is still a possibility for the shape to self-intersect non-locally (without singularity).

2.8.2 Skeletal Structures

One way to simplify the construction of a shape from a skeleton is to relax some of the conditions that are associated to medial axes. Skeletal structures, which we briefly describe now, have been introduced in [57, 58, 59] with this idea in mind.

There are two parts in Damon's skeletal structure. The first one is the skeletal set (the skeleton), which is a union of smooth open curves that meet at singular points (branching points or end-points) with well-defined tangents at their extremities.

The second part of the skeletal structure is the vectors which correspond to $r\rho$ in our previous notation, with some smoothness and consistency conditions; referring to [57] for details, here are the most important ones. Like with the medial axis, each point in the smooth curves of the skeletal set carries two of these vectors (one on each side of the curve), and singular points can carry one vector (end-points) or more than two at branching points. When one continuously follows one of these vectors along a smooth branch until a branching point, it must have a limit within the set of vectors at this point, and all vectors at this point can be obtained by such a process. At end-points, there is a unique vector which is tangent to the curve.

To summarize, a skeletal structure requires a skeletal set, say S, and, at each point p in the skeletal set, a set $U(p)$ of vectors that point to the generated curve, subject to the previous conditions. The generated curve itself is simply

$$C = \{p + U(p), p \in S\}\,.$$

The medial axis transform does induce a skeletal structure, but has additional properties, including the facts that, at each p, all vectors in $U(p)$ must have the same norm, and if p is on a smooth curve, the difference between the two vectors in $U(p)$ must be perpendicular to the curve. These properties are not required for skeletal structures.

Most of the analysis done in the previous section on the regularity of the generated curve with the medial axis transform can be carried over to skeletal structures. Along any smooth curve in the skeletal structure, one can follow a smooth portion of the generated curve, writing

$$x(u) = m(u) + r(u)\rho(u)$$

and assuming an arc-length parametrization in $m(u)$. Letting $c = -\dot{m}_u^T \dot{\rho}_u$, we can write, for some $\alpha \in \mathbb{R}$,

$$\dot{\rho}_u = -c\dot{m}_u + \alpha\rho$$

because ρ is assumed to be non-tangent to the skeletal set (except at its end-points). This definition of c generalizes the one given for the medial axis, in which we had $\dot{\rho}_u = -ch = -c\dot{m}_u + c\dot{\rho}_u\rho$. Since we have $\dot{x}_u = (1-cr)\dot{m}_u + (\alpha + \dot{r}_u)\rho$, we see that $cr < 1$ is here also a sufficient condition for the regularity of the curve.

We need to check that different pieces of curves connect smoothly at branching points. With the medial axis, a first-order contact (same tangents) was guaranteed by the fact that the generated curve was everywhere perpendicular to ρ. With skeletal structures, we have (since $\dot{\rho}_u^T\rho = 0$)

$$\dot{x}_u^T\rho = \dot{m}_u^T\rho + \dot{r}_u.$$

So, a sufficient condition for smooth contacts at branching points and at end-points is that $\dot{r}_u + \dot{m}_u^T\rho$ vanishes at the extremities of the smooth curves (while this quantity vanishes everywhere with the medial axis transform).

Obviously, these conditions are much less constraining than those associated to the medial axis transform. One can start fixing ρ, which defines c, then r such that $rc < 1$, with a few end-point conditions that must be satisfied. This simplification that is brought to curve generation, however, comes with a price, which is that a skeletal structure is not uniquely specified by a given curve, as the medial axis transform was. It cannot really be qualified as a "curve representation" like the ones we have considered so far.